Human pluripotent stem cell-derived eosinophils reveal potent cytotoxicity against solid tumors

Weifeng Lai,[1,4] Huangfan Xie,[1,4] Yuting Liu,[2] Feng Zheng,[1] Yingfeng Zhang,[1] Qi Lei,[1] Lejun Lv,[1] Jiebin Dong,[1] Jian Song,[1] Xue Gao,[1] Ming Yin,[3] Chengyan Wang,[1,*] and Hongkui Deng[1,*]

[1]School of Basic Medical Sciences, State Key Laboratory of Natural and Biomimetic Drugs, Peking University Health Science Center, and the MOE Key Laboratory of Cell Proliferation and Differentiation, College of Life Sciences, Peking-Tsinghua Center for Life Sciences, Peking University, Beijing 100191, China
[2]Center for Bioinformatics, School of Life Sciences, Center for Statistical Science, Peking University, Beijing 100871, China
[3]Beijing Vitalstar Biotechnology, Beijing 100012, China
[4]These authors contributed equally
*Correspondence: chengyanw@pku.edu.cn (C.W.), hongkui_deng@pku.edu.cn (H.D.)
https://doi.org/10.1016/j.stemcr.2021.06.005

SUMMARY

Eosinophils are attractive innate immune cells to use to potentiate T cell antitumor efficacy because they are capable of infiltrating tumors at early stages and modulating the tumor microenvironment. However, the limited number of functional eosinophils caused by the scarcity and short life of primary eosinophils in peripheral blood has greatly impeded the development of eosinophil-based immunotherapy. In this study, we established an efficient chemically defined protocol to generate a large quantity of functional eosinophils from human pluripotent stem cells (hPSCs) with nearly 100% purity expressing eosinophil peroxidase. These hPSC-derived eosinophils transcriptionally resembled their primary counterpart. Moreover, hPSC-derived eosinophils showed competent tumor killing capacity in established solid tumors. Furthermore, the combination of hPSC-derived eosinophils with CAR-T cells exhibited potential synergistic effects, inhibiting tumor growth and enhancing mouse survival. Our study opens up new avenues for the development of eosinophil-based immunotherapies to treat cancer.

INTRODUCTION

Adaptive T cell therapy has made breakthroughs in hematologic malignancies (Guedan et al., 2019). However, it still remains challenging for solid tumor treatment because of the barrier that prevents T cells from infiltrating the tumor and the immunosuppressive microenvironment (Majzner and Mackall, 2019). Increasing studies have demonstrated that innate immune cells play crucial roles in inducing the T cell immunity response and regulating the tumor microenvironment, which makes them promising innate immune cells for potentiating T cell antitumor efficacy (Demaria et al., 2019).

Among the different innate immune cell types, eosinophils are attractive immune effector cells because of their potential for improving immunotherapies. Eosinophils possess the unique advantage of quickly infiltrating tumors in the early response (Carretero et al., 2015; Reichman et al., 2016). After infiltration of tumors, eosinophils express multiple chemokine and alarmin receptors that allow them to orchestrate antitumor immunity from the following different aspects: first, infiltrated eosinophils could enhance the infiltration of antigen-specific T cells into the tumors (Carretero et al., 2015); second, they can regulate the tumor microenvironment with antitumorigenic properties; and third, they can produce dendritic cell and T helper cell chemoattractants (Rosenberg et al., 2013). Aside from the above studies in the mouse model, an increasing number of clinical studies show that the high efficiency of eosinophil infiltration of tumors correlates with a better prognosis in certain solid tumors (Gebhardt et al., 2015; Prizment et al., 2016; Weide et al., 2016). Moreover, eosinophils display antitumorigenic activity *in vitro* that is mediated by secretory granules (Spencer et al., 2014). The above studies have demonstrated that eosinophils hold great promise as a new type of immunotherapeutic cell for cancer treatment.

To develop eosinophil-based immunotherapy, one prerequisite is to generate a large number of functional human eosinophils. However, eosinophils are present in rather low numbers in peripheral blood, representing less than 3% of the total population of leukocytes (Weller and Spencer, 2017), and their half-life is comparatively short, ranging from 18 h to several days (Rosenberg et al., 2013). To resolve the shortage problem of functional eosinophils, one promising strategy is to generate unlimited numbers of functional mature eosinophils from human pluripotent stem cells (hPSCs).

In this study, we describe a highly efficient, chemically defined approach designed for just this purpose, based on our previously developed protocol for generating hematopoietic progenitor cells (HPCs) (Wang et al., 2012). We further show that these cells are able to directly kill various human tumor cells both *in vitro* and *in vivo* and demonstrate potential synergistic efficacy in suppressing established tumors by combining with CAR-T cells. Therefore, these hPSC-derived eosinophils could prove to be critical for the development of new strategies to facilitate cancer immunotherapy.

RESULTS

Efficient differentiation of eosinophils from human embryonic stem cells

The present protocol to generate eosinophils from human embryonic stem cells (hESCs) (H1) is modified from our previous study that produced HPCs from hPSCs (Wang et al., 2012). In our present method, we generated eosinophils in the order mesodermal progenitors, hemogenic endothelial cells, and HPCs using the specified differentiation media (Figure 1A).

We first monitored the generation of eosinophils from HPCs. CD34⁺CD45⁺ HPCs were generated and expanded from differentiation day 12 (E0) to differentiation day 16 (E4). These cells then gradually lost the expression of CD34 and became nearly completely CD34⁻CD45⁺ hematopoietic cells on E20 (Figure S1A). In the meantime, we traced the expression of the eosinophil-specific marker eosinophil peroxidase (EPX), which showed the earliest production of EPX⁺ cells on E4 (Figures 1B and 1C). On E20, 98% of cells in the final culture of differentiation were EPX⁺ cells (Figures 1B and 1C). Consistent with this, we found that the percentage of SSC^high cells gradually increased from 21.5% to 94.3% between E0 and E20, indicating a maturation of eosinophils with increasing level of cellular complexity (Figure S1B). We further analyzed the mature eosinophils and found that these cells expressed the active and mature eosinophil markers (Figure 1D). In addition, we further confirmed the expression of eosinophil-specific genes with immunostaining (Figures S1C and S1D). In parallel, basophil-specific genes could not be detected from E0 to E20 by immunostaining or RNA sequencing (RNA-seq) (Figures S1D and S1E). We next performed Giemsa staining and electron microscopy to further characterize these EPX⁺ cells. These cells displayed the typical features of eosinophils, possessing bilobed nuclei and abundant granules in the cytoplasm (Figure 1E). The granules of these cells were highly electron dense, consistent with the characteristics of granular proteins (Figure 1F). Eosinophils were generated at approximately 1,000-fold, that is, nearly 1,000 eosinophils were generated from a single initiating hESC (Figure 1G). Taken together, these results indicated that we successfully established a protocol that robustly generated eosinophils from hESCs with a high level of purity.

Transcriptional analysis of hESC-derived eosinophils

We next investigated the transcriptional fidelity of the eosinophil differentiation by conducting RNA-seq studies. Hierarchical clustering revealed that hESC-derived eosinophils (E20) clustered closely with primary naive eosinophils, and the differentiation process involved a PSC-to-eosinophil transition with a stage-specific clustering pattern (Figures 2A and 2B). Key eosinophil developmental regulators, such as the transcription factors *CEBPA*, *CEBPE*, *SPI1*, and *GATA1* (Reichman et al., 2016) and the receptors *IL5RA*, *CSF2RB*, *ADGRE1*, and *CD52* (Davis and Rothenberg, 2014), showed a gradual increase in expression from H1 to D32 (E20) eosinophils. Notably, the expression of the maturation marker *Siglec-8* (Rosenberg et al., 2013) was induced only at the later stages (Figure 2B). Compared with H1 cells, D32 (E20) eosinophils possessed high levels of the granular proteins *EPX*, *RNASE2*, *RNASE3*, *PRG2*, and *PRG3*, which are known to play pivotal roles in eosinophil cytotoxicity (Acharya and Ackerman, 2014) (Figure 2B). hPSC-derived eosinophils exhibited high expression levels of *IL5RA*, *CD244*, and *ITGB2* (*CD11b*) in the later stages (Figure 2B), of which CD244 can enhance antitumor effects by mediating eosinophil and natural killer cell degranulation (Lee et al., 2006). Impressively, the above genes were expressed in E20 hESC-derived cells at a level comparable to that seen in cord-blood-derived naive eosinophils.

To further confirm eosinophil-specific gene expression in the differentiated cells, we performed real-time qPCR on the induced cells on days 0 (H1), 12 (E0), 28 (E16), and 32 (E20) and on primary naive eosinophils (CB-E), and found that they exhibited high expression levels of *EPX*, *PRG2*, *PRG3*, *RNASE2*, *RNASE3*, and *IL5RA* in the later stages, comparable to primary naive eosinophils (Figure 2C).

We next performed Gene Ontology (GO) term and KEGG pathway analyses on the RNA-seq data. The most upregulated GO terms and pathways in day 32 (E20) eosinophils are shown in Figure 2D. As the results show, several pathways that are characteristic of innate immune responses were highly expressed in our induced eosinophils. In addition, these cells were highly associated with the terms "lysosome" and "lysosomal membrane," both of which are features of cells with large numbers of excretory granules. Taken together, the gene expression profiling strongly suggests a conversion of hESCs to fully competent eosinophils.

Functional assessment of the *in vitro* tumoricidal activity of hESC-derived eosinophils

We next assessed the tumoricidal properties of the hESC-derived eosinophils against three tumor cell lines: HCT116 (human colorectal carcinoma), MDA-MB-231 (human breast adenocarcinoma), and HepG2 (human hepatocellular carcinoma).

The H1-derived eosinophils exerted significant tumoricidal activity toward these tumor cells. Our data showed that H1-derived eosinophils showed competence in lysis ability of 40%–60% at 1:1 effector-to-target ratio, which was comparable to that of naive
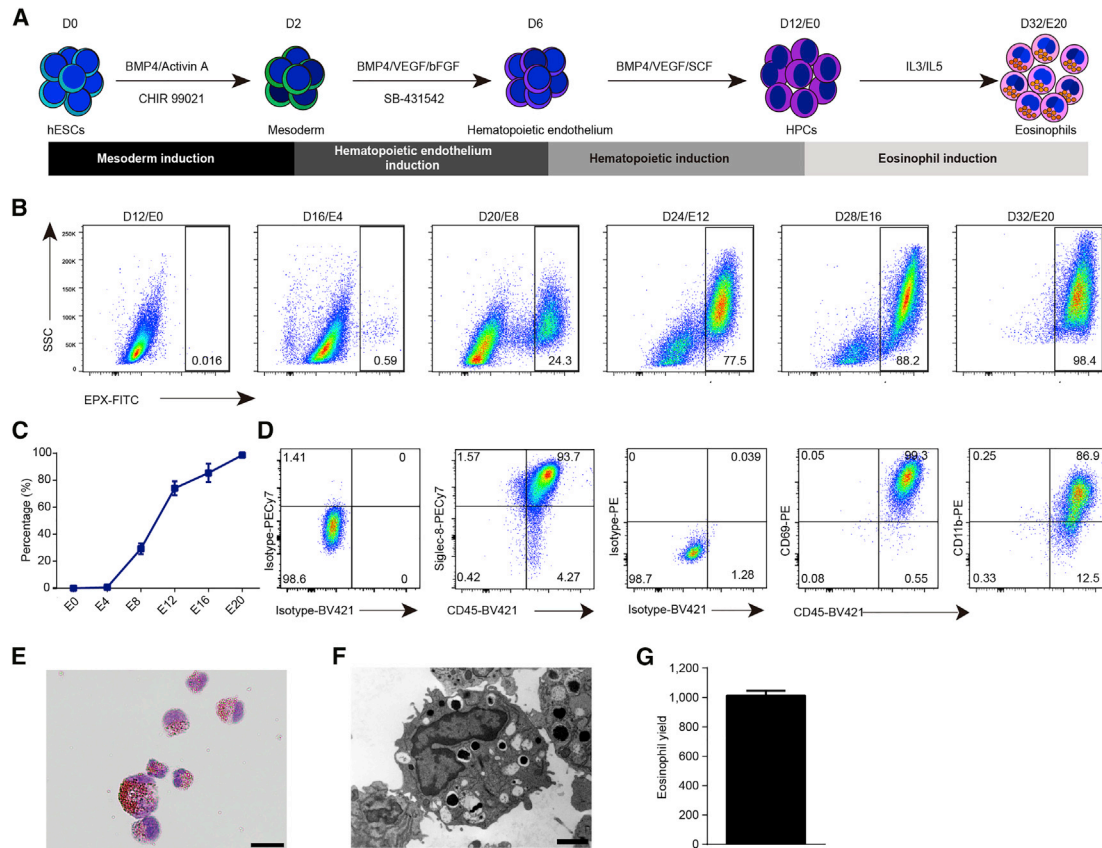
Figure 1. Efficient generation of eosinophils from hESCs

(A) Experimental schematic for the differentiation of hESCs into eosinophils.

(B) Representative flow plots from four independent experiments showing the generation of EPX$^+$ cells during eosinophil induction from E0 to E20.

(C) Percentage of EPX$^+$ cell population during the eosinophil induction process from starting H1 cells (n = 4 independent experiments). Data shown as the mean value ± SD.

(D) Representative flow plots from three independent experiments showing staining for the indicated surface marker on H1-derived eosinophils recovered on E20.

(E) Giemsa staining of induced cells recovered on E20. Scale bar, 20 μm.

(F) Electron microscope image of induced cells recovered on E16. Scale bar, 2 μm.

(G) Representative eosinophil yield at E16 from one H1 initiated cell (n = 3 independent experiments). Data shown as mean value ± SD.

See also Figure S1.

eosinophils (Figures 3A–3C). However, we did not observe the cytotoxicity of hPSC-derived eosinophils on human mesenchymal stem cells, human embryonic fibroblasts, or human umbilical vascular and endothelial cells (Figure S2A). These data demonstrate that hESC-derived eosinophils possessed highly specific cytotoxicity against tumor cells *in vitro*.

Functional assessment of the *in vivo* tumoricidal activity of hESC-derived eosinophils

To determine whether our hESC-derived eosinophils were capable of infiltrating tumors, we first injected H1-derived eosinophils into immunodeficient NPG mouse recipients that were preconditioned with human tumors formed by HCT116 cells by subcutaneous transplantation, and then analyzed the tumors at 48 h after eosinophil injection. Immunohistochemistry revealed that hESC-derived eosinophils (EPX$^+$ cells) infiltrated tumors (Figures S2B–S2D). By using flow cytometry analysis, we detected an apparent human CD45$^+$ cell population inside the tumors (Figure S2E), indicating that hESC-derived eosinophils are able to infiltrate tumors. Further, we tested the infiltration of hPSC-derived eosinophils in main organs and tissues, and the data showed a few hPSC-derived eosinophils detected in the spleen, but not in brain, heart, liver, lung, kidney, intestine, or colon (Figure S2F).
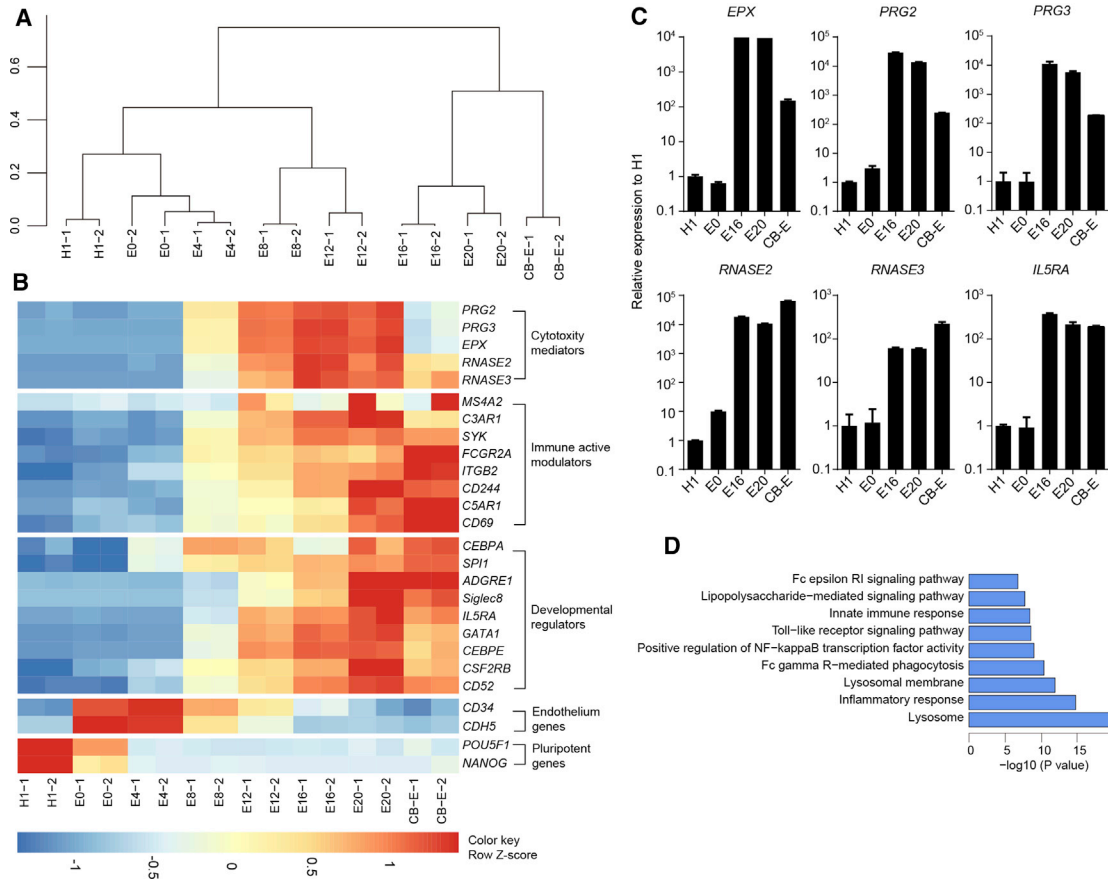
Figure 2. Transcriptional analysis of H1-derived eosinophils

(A) Dendritic hierarchical clustering of global gene expression of H1 cells and induced cells harvested on E0, E4, E8, E12, E16, and E20. Cord-blood-derived naive eosinophils (CB-E) were used as a positive control. Notably, the cells on E0 were sorted for CD34⁺ cell population for transcriptional analysis, while the whole cell culture was collected for transcriptional analysis on E4, E8, E12, E16, and E20. For cells at each time point, duplicate experiments were performed.

(B) Heatmaps of indicated gene expression, including cytotoxicity mediators, immune active modulators, developmental regulators, endothelium genes, and pluripotency genes in H1, CB-E, and induced cells harvested on E0, E4, E8, E12, E16, E20, and CB-E based on Z score from FPKM.

(C) Real-time qPCR analysis of key eosinophil gene expression in cells recovered on D0, E0, E16, and E20. Cord-blood-derived naive eosinophils (CB-E) were used as a positive control (n = 2). Data are shown as mean value ± SD. Similar results were obtained in three independent experiments.

(D) GO term and KEGG analysis showing GO terms and KEGG pathways that were upregulated in H1-derived eosinophils collected on E20 compared with H1.

We next investigated the *in vivo* antitumor activity of the hESC-derived eosinophils. We first inoculated tumor cells (HCT116) into immunodeficient NPG mouse recipients to establish tumor-xenograft models. Then we injected H1-derived eosinophils into the tumor-bearing mice (Figure 3D). As the bioluminescence imaging showed, the injection of eosinophils significantly inhibited tumor growth in HCT116-tumor-bearing mice (Figure 3E). The eosinophil infusion evidently prolonged the median survival time of the HCT116-tumor-bearing mice compared with the untreated group (Figure 3F). In addition, the infusion of eosin-

ophils significantly suppressed tumor growth (Figure S2G) and prolonged the median survival time of MDA-MB-231-tumor-bearing mice (Figure S2H). Taken together, these results demonstrate that hESC-derived eosinophils possess tumoricidal properties *in vivo*.

Next, we evaluated the tumoricidal efficacy of hESC-derived eosinophils in established tumors. HepG2 cells were injected into each mouse and 60–70 mm³ tumors were established on day 7 (Figures 4A and S2I). hESC-derived eosinophils were injected into tumor-bearing mice at the 7- and 10-day timepoints (Figure 4A). We found
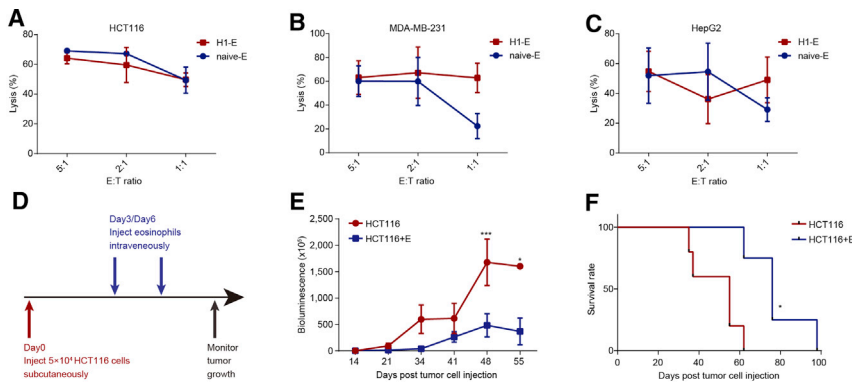
Figure 3. Potent cytotoxicity of hESC-derived eosinophils against solid tumors *in vitro* and *in vivo*

(A–C) Cytotoxicity of the H1-derived eosinophils (H1-E) and cord-blood-derived eosinophils (naive-E) toward HCT116 (A), MDA-MB-231 (B), and HepG2 (C) target cells at the indicated effector-to-target ratios (n = 3). The lysis rate of target cells is shown as the mean percentage value ± SD. n = 3 independent experiments.

(D) Schematic depicting the *in vivo* tumor assay.

(E) The HCT116 tumor cell burden of each group measured on the indicated days after tumor cell injection, as shown by bioluminescence imaging (n = 5 for control group; n = 4 for HCT116+E group). Statistical significance was assessed using two-tailed ANOVA, where *p < 0.05 and ***p < 0.001; data shown as mean values ± SEM.

(F) Kaplan-Meier curve representing the percentage survival of the experimental groups in the HCT116-xenograft mouse models (n = 5 for control group; n = 4 for HCT116+E group). Statistical analyses were calculated using log-rank (Mantel-Cox) test, where *p < 0.05. See also Figure S2.

that the injection of hESC-derived eosinophils significantly inhibited the tumor growth (Figures 4B and 4C). Similarly, hESC-derived eosinophils also exhibited significant tumor inhibition effects on HCT116 colorectal carcinoma (Figure S2J). We further detected the safety of hPSC-derived eosinophils in main organs or tissues by hematoxylin and eosin staining after injecting different doses of hPSC-derived eosinophils. No abnormal morphology was observed at the doses we tested (Figure S3A). Taken together, these data demonstrate that hESC-derived eosinophils possess competent cytotoxic effects suppressing tumor growth in established solid tumors.

hESC-derived eosinophils enhanced tumor killing capacity of CAR-T cells *in vivo*

CAR-T cells may lose their antitumor effects against solid tumors due to inactivation of CAR-T cells induced by the immune-suppressive microenvironment (Newick et al., 2017). We next studied whether hESC-derived eosinophils could facilitate CAR-T cell antitumor efficiency in established solid tumors. We generated CAR-T cells through transduction of the HER2 CAR gene into peripheral blood T cells (Figures S3B and S3C). Then, we injected the cells into the established tumor-bearing mice divided into three experimental groups: CAR-T cells alone, hESC-derived eosinophils alone, and the combination of hESC-derived eosinophils and CAR-T cells (Figure 4D). The results showed that all three experiment groups significantly inhibited tumor growth in HCT116 tumor-bearing mice compared with the control group (Figure 4E). These three experiment groups apparently extended the survival time of the HCT116-tumor-bearing mice compared with the control group (Figure 4F). In particular, we found that the combination of CAR-T cells and hESC-

derived eosinophils exhibited better antitumor effects against established tumors than CAR-T cells alone or hESC-derived eosinophils alone (Figures 4E, 4F, and S3D). Taken together, these results indicate a potential synergy of action when both eosinophils and CAR-T cells are used together.

Efficient differentiation of functional eosinophils from human iPSCs

We also generated EPX⁺ eosinophils from human induced pluripotent stem cells (iPSCs) (Figure S4A and S4E). Real-time qPCR showed that the induced cells at E20 displayed upregulation of eosinophil-specific genes compared with iPSCs (Figures S4B and S4F). Human iPSC-derived eosinophils also exhibited potent tumor killing capacity on HepG2 and HCT116 cells *in vitro* (Figures S4C and S4G) and significantly suppressed tumor growth *in vivo* (Figures S4D and S4H). All these data demonstrate that functional mature eosinophils that possess competent cytotoxic effects on solid tumors can be derived from independent human iPSCs.

DISCUSSION

Here, we report the successful development of a protocol to efficiently generate large numbers of eosinophils expressing eosinophil-specific granule proteins and genes from hPSCs. We also demonstrate that these hPSC-derived eosinophils possess a high degree of cytotoxicity against diverse tumor cells in both *in vitro* and *in vivo* settings. In particular, we found that the combination of hPSC-derived eosinophils with CAR-T cells presents higher efficiency of tumor killing *in vitro* and inhibits tumor growth more effectively *in vivo*.
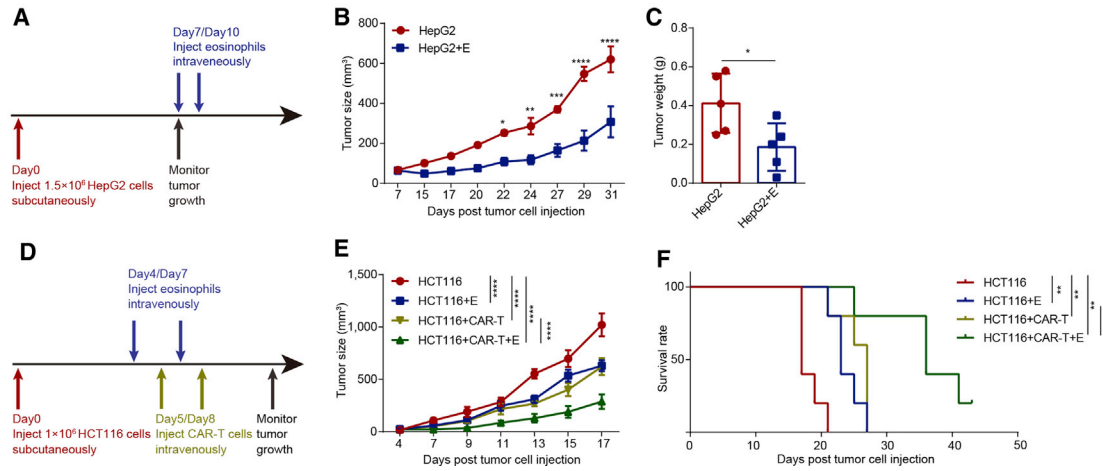
Figure 4. Enhanced tumoricidal activity of CAR-T cells against solid tumors by combination with hESC-derived eosinophils

(A) Schematic showing the *in vivo* tumor assay.

(B) HepG2 tumor size of each group was determined on the indicated days after tumor cell injection (n = 5 for each group). Statistical significance was assessed using two-tailed ANOVA, where *p < 0.05, **p < 0.01, ***p < 0.001, and ****p < 0.0001; data are shown as the mean values ± SEM.

(C) Tumor weight of HepG2 on day 32 (n = 5 for each group). Statistical significance was assessed using unpaired t test, where *p < 0.05, data are shown as the mean values ± SD.

(D) Schematic showing the *in vivo* tumor assay of CAR-T cells and hPSC-derived eosinophils.

(E) HCT116 tumor size of each group was measured on the indicated days after tumor cell injection (n = 5 for control group, CAR-T cell group, and combination group; n = 4 for hESC-derived eosinophil group). Statistical significance was assessed using two-tailed ANOVA compared with the HCT116 group, where ****p < 0.0001; data are shown as mean values ± SEM. These are representative data from two independent experiments.

(F) Kaplan-Meier curve representing the percentage survival of the experimental groups in the HCT116-xenograft mouse models (n = 5 for control group, CAR-T cell group, and combination group; n = 4 for hESC-derived eosinophil group). Statistical analyses were calculated using log-rank (Mantel-Cox) test, where*p < 0.05 and **p < 0.01. These are representative data from two independent experiments. See also Figures S3 and S4.

Notably, hPSC-derived eosinophils produced in our study displayed eosinophil-specific features comparable to those of naive eosinophils. In terms of morphological phenotype, they exhibited bilobed nuclei, acidophilic stain incorporation, and electron-dense granules. At the transcriptional level, they expressed receptors involved in eosinophil survival and signal transduction, such as *IL5RA* and *Siglec-8* (Rosenberg et al., 2013) at high levels. In addition, these eosinophils also expressed cytotoxic granular proteins such as *EPX*, *PRG2*, *PRG3*, *RNASE2*, and *RNASE3*, which are known to be critical for the function of eosinophils with tumoricidal properties (Acharya and Ackerman, 2014). Most importantly, hPSC-derived eosinophils exhibited strong tumor killing activity, characteristic of naive eosinophils. Eosinophils lack surface T cell receptors and so should not cause graft-versus-host disease. With the advantage of hPSCs' ability to be genetically manipulated to establish HLA-deficient universal stem cells (Deuse et al., 2019), hPSC-derived eosinophils hold great potential as a universal, "off-the-shelf" cell source for immunotherapy.

Another advantage of our study is the development of a chemically defined approach to generate large quantities of functional human eosinophils from hPSCs. Although previous studies showed that hPSC-derived myeloid progenitors could generate MBP⁺ eosinophils (Choi et al., 2009), these studies relied on stromal cells and serum, as well as the purification of hematopoietic progenitors. More importantly, EPX⁺ eosinophils could be generated at a high purity and in large quantities, with nearly 1,000-fold increase from starting cells in number. Therefore, this protocol possesses multiple advantages that make it more suitable for future clinical applications.

Our study is the first report to demonstrate competent *in vivo* antitumor activity of hPSC-derived eosinophils and showed potential to facilitate CAR-T cell effects against solid tumors. According to the *in vivo* data for evaluating antitumor activity, hPSC-derived eosinophils exhibited strong efficacy, not only in inoculated tumors, but also in established tumors. Compared with other immune cell types, the major advantages of eosinophils' application in immunotherapy would be their capacity to respond at an

early stage and quickly infiltrate tumors, which could facilitate the attraction of T cells and regulate the tumor microenvironment to potentiate the T cell antitumor activity (Carretero et al., 2015). Our data showed that the combination of hPSC-derived eosinophils and CAR-T cells significantly inhibited tumor growth *in vivo*. This potential synergistic efficacy may result from the eosinophils' unique advantage of quick infiltration of tumors at the early response based on their expression of multiple chemokine and alarmin receptors (Carretero et al., 2015; Reichman et al., 2016). Their early infiltration of the tumor allowed the regulation of the tumor microenvironment with anti-tumorigenic properties or produced dendritic cell and T helper cell chemoattractants (Rosenberg et al., 2013). The eosinophils could directly lyse tumor cells, resulting in enhanced alarmin signals or chemokine secretion to enhance the infiltration of antigen-specific T cells into the tumors (Carretero et al., 2015). These features may potentiate the enhanced synergistic antitumor efficacy exhibited by CAR-T cells, and the underlying mechanisms are worth further study.

In summary, our study provides a robust method for generating unlimited numbers of functional human eosinophils for enhancing T cell antitumor activity, and this could represent an important step toward developing novel strategies of combining CAR-T cells with other immune cells for cancer immunotherapy.

EXPERIMENTAL PROCEDURES

Eosinophil differentiation from hESCs and iPSCs

hESCs (H1) and iPS cells (iPS-#7, iPS-#8) were cultured in Matrigel-coated plates at low density. Activin A, BMP4, and CHIR99021 were used to induce mesoderm. BMP4, VEGF, bFGF, and SB-431542 were used to induce hemogenic endothelial cells. BMP4, VEGF, SCF, NAC, and minocycline hydrochloride were used to induce HPCs. IL-3 and IL-5 were used to induce eosinophils. A detailed description is provided in the supplemental experimental procedures.

In vitro cytotoxicity assays

Tumor cells were seeded in 96-well plates. Six to ten hours later, the eosinophils were added to the target cells. After incubation for 20 h, the apoptotic cells of the tumor target cells were quantified by a standard bioluminescence assay. A detailed description is provided in the supplemental experimental procedures.

In vivo tumor assay

Luciferase-marked target cells were injected subcutaneously into recipient NPG mice, followed by two intravenous injections of E16–E20 hPSC-derived eosinophils. For established tumors, tumor cells were injected subcutaneously and eosinophils were injected intravenously. For evaluating the combination effects of CAR-T and hESC-derived eosinophils, tumor cells were injected subcuta-neously. Two intravenous injections of eosinophils, CAR-T cells, or their combination were performed. A detailed description is provided in the supplemental experimental procedures.

Statistical analysis

Statistical analysis was performed with GraphPad Prism software. Data are shown as the means with standard deviation or means with standard error of the mean. Comparisons between groups were assessed using unpaired t test or two-tailed ANOVA as indicated. For all analyses, $p < 0.05$ was considered statistically significant. The statistical significance and n values are described in the figure legends. All the flow analysis data were processed with FlowJo v.10 software.

Data and code availability

RNA-seq data of this study have been deposited in the GEO database under accession no. GSE148907.

REFERENCES

Acharya, K.R., and Ackerman, S.J. (2014). Eosinophil granule proteins: form and function. J. Biol. Chem. *289*, 17406–17415.

Carretero, R., Sektioglu, I.M., Garbi, N., Salgado, O.C., Beckhove, P., and Hammerling, G.J. (2015). Eosinophils orchestrate cancer rejection by normalizing tumor vessels and enhancing infiltration of CD8(+) T cells. Nat. Immunol. *16*, 609–617.

Choi, K.D., Vodyanik, M.A., and Slukvin, I.I. (2009). Generation of mature human myelomonocytic cells through expansion and differentiation of pluripotent stem cell-derived lin-CD34+CD43+CD45+ progenitors. J. Clin. Invest. *119*, 2818–2829.

Davis, B.P., and Rothenberg, M.E. (2014). Eosinophils and cancer. Cancer Immunol. Res. *2*, 1–8.

Demaria, O., Cornen, S., Daeron, M., Morel, Y., Medzhitov, R., and Vivier, E. (2019). Harnessing innate immunity in cancer therapy. Nature *574*, 45–56.

Deuse, T., Hu, X., Gravina, A., Wang, D., Tediashvili, G., De, C., Thayer, W.O., Wahl, A., Garcia, J.V., Reichenspurner, H., et al. (2019). Hypoimmunogenic derivatives of induced pluripotent stem cells evade immune rejection in fully immunocompetent allogeneic recipients. Nat. Biotechnol. *37*, 252–258.

Gebhardt, C., Sevko, A., Jiang, H., Lichtenberger, R., Reith, M., Tarnanidis, K., Holland-Letz, T., Umansky, L., Beckhove, P., Sucker, A., et al. (2015). Myeloid cells and related chronic inflammatory factors as novel predictive markers in melanoma treatment with ipilimumab. Clin. Cancer Res. *21*, 5453–5459.

Guedan, S., Ruella, M., and June, C.H. (2019). Emerging cellular therapies for cancer. Annu. Rev. Immunol. *37*, 145–171.

Lee, K.M., Forman, J.P., McNerney, M.E., Stepp, S., Kuppireddi, S., Guzior, D., Latchman, Y.E., Sayegh, M.H., Yagita, H., Park, C.K., et al. (2006). Requirement of homotypic NK-cell interactions through 2B4(CD244)/CD48 in the generation of NK effector functions. Blood *107*, 3181–3188.

Majzner, R.G., and Mackall, C.L. (2019). Clinical lessons learned from the first leg of the CAR T cell journey. Nat. Med. *25*, 1341–1355.

Newick, K., O'Brien, S., Moon, E., and Albelda, S.M. (2017). CAR T cell therapy for solid tumors. Annu. Rev. Med. *68*, 139–152.

Prizment, A.E., Vierkant, R.A., Smyrk, T.C., Tillmans, L.S., Lee, J.J., Sriramarao, P., Nelson, H.H., Lynch, C.F., Thibodeau, S.N., Church, T.R., et al. (2016). Tumor eosinophil infiltration and improved survival of colorectal cancer patients: Iowa Women's Health Study. Mod. Pathol. *29*, 516–527.

Reichman, H., Karo-Atar, D., and Munitz, A. (2016). Emerging roles for eosinophils in the tumor microenvironment. Trends Cancer *2*, 664–675.

Rosenberg, H.F., Dyer, K.D., and Foster, P.S. (2013). Eosinophils: changing perspectives in health and disease. Nat. Rev. Immunol. *13*, 9–22.

Spencer, L.A., Bonjour, K., Melo, R.C., and Weller, P.F. (2014). Eosinophil secretion of granule-derived cytokines. Front. Immunol. *5*, 496.

Wang, C., Tang, X., Sun, X., Miao, Z., Lv, Y., Yang, Y., Zhang, H., Zhang, P., Liu, Y., Du, L., et al. (2012). TGFbeta inhibition enhances the generation of hematopoietic progenitors from human ES cell-derived hemogenic endothelial cells using a stepwise strategy. Cell Res. *22*, 194–207.

Weide, B., Martens, A., Hassel, J.C., Berking, C., Postow, M.A., Bisschop, K., Simeone, E., Mangana, J., Schilling, B., Di Giacomo, A.M., et al. (2016). Baseline biomarkers for outcome of melanoma patients treated with pembrolizumab. Clin. Cancer Res. *22*, 5487–5496.

Weller, P.F., and Spencer, L.A. (2017). Functions of tissue-resident eosinophils. Nat. Rev. Immunol. *17*, 746–760.